DTU Library

A-, B- and C-type prymnesins are clade specific compounds and chemotaxonomic markers in Prymnesium parvum

Binzer, Sofie Bjørnholt; Svenssen, Daniel Killerup; Daugbjerg, Niels; Alves-de-Souza, Catharina; Pinto, Ernani; Hansen, Per Juel; Larsen, Thomas Ostenfeld; Varga, Elisabeth

Link back to DTU Orbit

A-, B- and C-type prymnesins are clade specific compounds and chemotaxonomic markers in *Prymnesium parvum*

Sofie Bjørnholt Binzer[a,1], Daniel Killerup Svenssen[b,1], Niels Daugbjerg[c,*],
Catharina Alves-de-Souza[d,e], Ernani Pinto[f], Per Juel Hansen[a,*], Thomas Ostenfeld Larsen[b,*],
Elisabeth Varga[b]

[a] *Marine Biological Section, Department of Biology, University of Copenhagen, Strandpromenaden 5, 3000, Helsingør, Denmark*
[b] *Department of Biotechnology and Biomedicine, Technical University of Denmark, Søltofts Plads 221, 2800, Kgs. Lyngby, Denmark*
[c] *Marine Biological Section, Department of Biology, University of Copenhagen, Universitetsparken 4, 2200, Copenhagen K, Denmark*
[d] *Algal Resources Collection, MARBIONC at CREST Research Park, University of North Carolina Wilmington, 5600 Marvin K. Moss Ln, Wilmington, NC, 28409, USA*
[e] *Laboratório de Ficologia, Departamento de Botânica, Museu Nacional/Universidade Federal do Rio de Janeiro, Quinta da Boa Vista S/N, São Cristóvão, Rio de Janeiro, RJ, 20940–040, Brazil*
[f] *School of Pharmaceutical Sciences, University of Sao Paulo, Av. Prof Lineu Prestes 580, 05508-000, São Paulo, SP, Brazil*

ARTICLE INFO

ABSTRACT

Harmful blooms formed by planktonic microalgae (HABs) in both freshwater and coastal waters regularly lead to severe mortalities of fish and invertebrates causing substantial economic losses of marine products worldwide. The mixotrophic haptophyte *Prymnesium parvum* is one of the most important microalgae associated with fish kills. Here 26 strains of *P. parvum* with a wide geographical distribution were screened for the production of prymnesins, the suspected causative allelochemical toxins. All investigated strains produced prymnesins, indicating that the toxins play an important role for the organism. The prymnesins can be classified into three types based on the length of the carbon backbone of the compound and each algal strain produced only one of these types. Biogeographical mapping of the prymnesin distribution indicated a global distribution of each type. In addition, phylogenetic analyses based on internal transcribed spacer (ITS) sequences revealed monophyletic origin of all prymnesin types and clades could therefore be defined based on the toxic compound. It might be that evolution of new species within the *P. parvum* species complex is driven by changes in toxin type or that they are a result of it. Such a correlation between chemotype and phylotype has never been documented before for a harmful microalga. Chemotaxonomy and ITS-type classification may thus be used to further delimit the *P. parvum* species complex.

1. Introduction

Increased nutrient loading and exploitation of aquatic ecosystems for recreation and human food production has enlarged the pressure on aquatic ecosystems over the past 60 years. The nutrient enrichment has been discussed as one factor responsible for the increase in harmful

algal blooms (HABs), which in the worst cases have caused severe mortalities of fish and shellfish and thereby huge economic losses to the aquaculture industry (Anderson et al., 2000; Sanseverino et al., 2016). The detrimental effects of HABs are mainly due to the production and excretion of highly toxic compounds, often referred to as allelochemicals. This has sparked an increased interest in the mechanisms that

trigger HABs and their toxicity.

Allelochemicals are excreted to the surrounding water and act on e.g. cell membranes leading to effects such as cell immobilization and lysis, affecting a wide range of organisms including competitors and grazers. The allelochemicals may also affect larger animals, (e.g. fish Kaartvedt et al., 1991; Edvardsen and Paasche, 1998) and are then often referred to as ichthyotoxins. Here the more general term allelo-chemicals will be used. Many suggestions of the adaptive significance of the allelochemicals have been put forward and also how and why they have evolved (Jonsson et al., 2009; Ianora et al., 2011). Eukaryote microalgae that produce allelochemicals tend to be mixotrophic, com-bining photosynthesis and food uptake. They are able to consume or-ganisms that are frequently much larger than the algae themselves (Tillmann, 2003; Berge et al., 2012). Thus, microalgae do not only benefit from killing competitors and grazers, but also exploit them for food.

The best studied allelopathic microalgae are the haptophyte *Prymnesium parvum* and the dinoflagellates *Karlodinium veneficum* and *K. armiger*. In these cases, the causative compounds have been identified as large polyethers (Igarashi et al., 1996, 1999; Van Wagoner et al., 2008; Peng et al., 2010; Rasmussen et al., 2016b, 2017). Interestingly, each of these toxins seems to be exclusively produced by a single spe-cies. For example, karlotoxin is only produced by *K. veneficum*, while the newly described karmitoxin is only found in the closely related species *K. armiger* (Rasmussen et al., 2017). The difference between these compounds lies mainly in the different length of the core-carbon backbone of the molecule. Recently it was discovered that the hapto-phyte *P. parvum* produces three different types of prymnesins, also distinguished by the length of the carbon backbone of the molecule (Rasmussen et al., 2016b). In the study by Rasmussen et al. (2016b) 10 strains were investigated, and it was observed that each strain ex-clusively produced one of the three types and never a combination thereof.

Two phylogenetic studies of *P. parvum* have been published pre-viously based on the internal transcribed spacer 1 (ITS-1). These in-cluded 12 and 23 strains of *P. parvum* from around the world and they identified two and three major clades, respectively (Larsen and Medlin, 1997; Lutz-Carrillo et al., 2010). The latter of these studies indicated that the strains of *P. parvum* were not restricted in their global dis-tribution indicating great dispersal and colonization potential (Lutz-Carrillo et al., 2010). The recent discovery of three prymnesin types in combination with the identification of three distinct lineages of *P. parvum* raises the question whether or not the production of A-, B- and C-type prymnesins matches the evolutionary history of *P. parvum* based on analysis of ITS sequences.

The aim of the present work has been to explore 26 strains of *P. parvum* that had been isolated from around the world to characterize: 1) the prymnesin toxin type of each strain using high resolution mass spectrometry and 2) infer the phylogeny of the strains using complete ITS sequences (ITS-1 and ITS-2) and map onto the tree topology the type of prymnesins produced for each strain. The data will reveal if: (A) a single strain produces more than one type of prymnesin; (B) more than three different types of prymnesins can be identified; (C) a bio-geographical pattern exist with regard to the distribution of prymnesin types; (D) the production of A-, B- and C-type prymnesins is related to phylogeny of *P. parvum* based on ITS sequences. This will allow us to discuss the possible evolution of the prymnesin types and evaluate the validity of splitting the species *P. parvum* into several species using chemotaxonomy and ITS-type classification.

2. Materials and methods

2.1. Cultivation of P. parvum cultures

Twenty-six isolates identified as *P. parvum* were obtained from dif-ferent culture collections (see Table S1 for details): *P. parvum* PPDW02

and PPSR01 isolates were kindly provided by Gustaaf Hallegraeff (University of Tasmania) and *P. parvum* ARC479 (http://www.algalresourcescollection.com/arc479) was previously isolated and characterized by Alves-de-Souza et al. (2017).

Depending on the original salinity of the strains F/2 media (Guillard, 1975) with salinity of ca. 30 or 9 were used. Media were prepared with seawater sampled from below the pycnocline off the coast of Helsingør (Denmark) and sterilized (90 min at 95 °C) before use. Media with a salinity of 9 were prepared by mixing seawater (salinity of ca. 30) with demineralized water and $NaHCO_3$ was added (28 mL 0.5 M to 10 L medium) in order to compensate for the lack of inorganic carbon in demineralized water. All cultures were kept at a temperature of 15 °C and light was provided with an intensity of 150 µmol photons $m^{-2}s^{-1}$ and a light:dark cycle of 14:10 h. For screening purposes, 1 L bottles were inoculated with an initial concentration of ca. 50 000 cells mL^{-1} and gently aerated during cultivation. The con-centrations were determined every 2–3 days by counting the cells fixed with acidic Lugol's (VWR Chemicals, Radnor, PA, USA) (2% final con-centration) using a Sedgewick Rafter chamber and an inverted micro-scope (Olympus CKX53, London, United Kingdom). The cultures were harvested during their late exponential growth phase at cell con-centrations between 390 000 to 1 200 000 cells mL^{-1}.

The Brazilian strain of *P. parvum* was cultivated in a 10 L photo-bioreactor (IKA Algaemaster 10 control, IKA® Works Inc., Wilmington, NC, USA) at 20 °C, 70 µmol $m^{-2}s^{-1}$ and a 12:12 dark:light photoperiod (LED Light). Air bubbling and CO_2 injection was used to maintain a pH of ca. 8. For inoculation 200 mL of a 100 000 cells mL^{-1} dense culture was added in 9.8 L of L1 media at a salinity of 20 to have an initial concentration of 1 000 cells mL^{-1}. After 2 weeks, the culture was harvest by centrifugation when it reached 190 000 cells mL^{-1}.

2.2. Harvest of biomass and extraction procedure

The biomasses were harvested by centrifugation on a Sigma 3–18 K centrifuge (Sigma Laborzentrifugen GmbH, Osterode am Harz, Germany) for 15 min at 4 700 RPM (ca. 4 220*g*) and 4 °C and the su-pernatants were discarded. The Brazilian strain was harvested with a Sorvall superspeed RC2-B centrifuge at 4 °C and 12 000*g*. Samples were stored at -20 °C overnight or at −80 °C for several days.

The biomass pellets were thawed and extracted twice with cold acetone (-20 °C; 20 mL each) for removing among others chlorophylls. After vortexing centrifugation was performed with the same settings as described above for harvesting the biomass. The supernatants of both centrifugation steps were pooled in a new polypropylene tube (acetone extract). After the chlorophyll extraction the biomass was extracted twice with MeOH (20 mL each) and sonication in an ultrasonic bath for 30 min (sweep mode). After centrifugation (15 min, 4 220*g*, 4 °C) the supernatants were pooled in a new polypropylene tube (MeOH extract). Both extracts (acetone and MeOH) were concentrated to dryness under nitrogen at 35 °C, reconstituted in 1 mL MeOH and transferred to a glass HPLC vial.

2.3. LC-DAD-HRMS analysis

Separation was performed on an Ultimate 3000 ultra-high perfor-mance liquid chromatographic system (UHPLC) (Dionex, Sunnyvale, CA, USA) using a 100 x 2 mm, 2.6 µm Kinetex C18 column (Phenomenex, Aschaffenburg, Germany) at 40 °C A linear water-acet-onitrile gradient, containing 20 mM formic acid, from 10% to 100% acetonitrile in 10 min and maintained for 2 min before returning to the start conditions at a flow rate of 0.4 mL min^{-1} was applied. The samples were maintained at 8 °C in the autosampler and 5 µL was injected for each analysis.

An Ultimate 3000 Diode Array Detector (DAD, Dionex) was used for acquiring UV/vis data in a wavelength range from 200 nm to 700 nm. High resolution mass spectrometric (HRMS) data were acquired on a

MaXis HD quadrupole time-of-flight mass spectrometer (QTOF-MS) (Bruker Daltonik, Bremen, Germany). The mass spectrometer was operated in positive mode with a capillary voltage of 4 500 V recording data in a scan range from m/z 300 to 2 500 at a rate of 2 scans per second. Drying gas flowrate was set to $10.0 \, L \, min^{-1}$, the temperature to 200 °C and the nebulizer pressure was 180 kPa. To accommodate larger ions the following settings were used for the collision cell: transfer time 100 µs, collision cell RF 1 500 Vpp, and pre-pulse storage 10 µs. The mass range was calibrated using sodium formate.

2.4. Data evaluation

The acquired data were evaluated based on three different principles: First, a search list containing the 16 molecular features described in Rasmussen et al. (2016) was applied in DataAnalysis Ver. 4.2 (Bruker Daltonik) and continuously expanded during the study as soon as novel prymnesin-like compounds were tentatively identified. At the end of the study, theoretical sum formulas were calculated based on the results: backbones with one double bond more (hence one degree higher saturation) and all sugar combinations (one or two pentose or hexose units, or combinations thereof). Finally, all samples were retrospectively reanalyzed with the newly created list. Secondly, the software tool Dynamic Cluster Analysis (DCAnalysis Ver. 1.09, available at http://www.bioengineering.dtu.dk/english/researchny/platforms/metabolom/lc-hrmsfiltering, Andersen et al., 2016) with the following settings was applied: retention time drift 1.0 s, mass error 3 ppm, applied filter DCA-Hal, area cut-off 500 000, feature mode "Molecular", and required rate 100%. Thirdly, data were manually investigated based on the UV/vis chromatogram at 280 nm.

2.5. DNA extraction and PCR amplification

Total genomic DNA was extracted from the 26 cultures of *P. parvum* (Table S1) using the PowerPlant Pro DNA Isolation kit following the manufacturer's instructions (MO BIO Laboratories Inc, Carlsbad, CA, USA). To amplify the Internal Transcribed Spacers (ITS 1 and 2) of the ribosomal cistron (ca. 700 base pairs) two primers (ITS 1 and ITS 4) originally designed by White et al. (1990) were used. The PCR amplification kit used was 5X Hot FIREPol Blend Master Mix (Solit Biodyne, Tartu, Estonia) and PCR conditions were one initial cycle of denaturation at 95 °C for 12 min followed by 35 cycles each consisting of denaturation at 95 °C for 30 s, annealing at 54 °C for 30 s and extension at 72 °C for 40 s A final step included extension at 72 °C for 5 min. Electrophoresis in 1.5% agarose-casted gels was used to confirm the expected length of Gelred stained PCR products. Visualization of products used a gel documentation XR System from BioRad (Hercules, CA, USA). Fragment length was evaluated by comparison to a 100-base-pair RAINBOW eXtended DNA ladder (BIORON, GmhB, Ludwigshafen, Germany).

Amplified DNA fragments were purified using ultrafiltration by applying the Nucleofast 96 kit from Macherey-Nagel (GmbH & Co, KG, Düren, Germany) following the manufacturer's recommendations. The ITS sequences (including 5.8S rDNA) were determined in both directions using the amplifications primers. The service provided by Macrogen (Amsterdam, Netherland) was used for sequence determinations. The sequences were deposited in GenBank (https://www.ncbi.nlm.nih.gov/genbank/) and accession numbers are provided in Table S2.

2.6. Phylogenetic inference

The phylogeny of *P. parvum* cultures was inferred by analysis of 696 base-pairs including introduced gaps. Sequences were aligned using ClustalW and further edited in Jalview (ver. 14, Waterhouse et al., 2009). The resulting data matrix was analyzed using Bayesian (BA) and maximum likelihood (ML). For BA MrBayes (ver. 3.2.5 × 64, Ronquist and Huelsenbeck, 2003) with a total of $10*10^6$ generations and a sampling frequency of trees for every 1 000 generations was used. Evaluation of the burn-in value was by plotting lnL scores as a function of generations and a burn-in was reached after 1 001 000 (conservative estimate). This left 9000 trees for construction of a 50% majority-rule consensus tree. jModeltest (ver.2.1.3, Darriba et al., 2012) was used to obtain the parameter settings for ML analysis and the GTR-I-G was chosen as the best fit model for the ITS and 5.8S rDNA based data matrix. In total 88 different models were examined and for ML analysis the online version of PhyML (Guindon et al., 2010) available at the Montpellier bioinformatics platform was used. The robustness of the tree topology was evaluated with 1 000 bootstrap replications. *Platychrysis pigra*, another member within the order Prymnesiales, was used as the outgroup in both phylogenetic analyses.

3. Results

3.1. Screening of P. parvum strains for A, B, and C-type prymnesins

A total of 26 *P. parvum* strains were screened using LC-DAD-HRMS. The UV/vis data were used to identify the presence of prymnesins and HRMS to confirm the presence and specific type of prymnesins. The prymnesins with an UV-signal at 280 nm eluted in a retention time window from 4 to 7 min, starting with C-type prymnesins (4.5–5.7 min), followed by B-type prymnesins (5.7–6.3 min), and lastly A-type prymnesins (6.2–6.5 min), see Fig. S1. Hence the retention time of the UV-signal already provided a hint which prymnesin type is present, but HRMS was required to confirm the identity. Each prymnesin type is defined by the number of carbon atoms in the aglycone backbone based on the HRMS-data and derived sum formulas. A-type prymnesins are the largest with 91 carbons, while the backbone of B- and C-type prymnesins contains 85 and 83 carbons, respectively
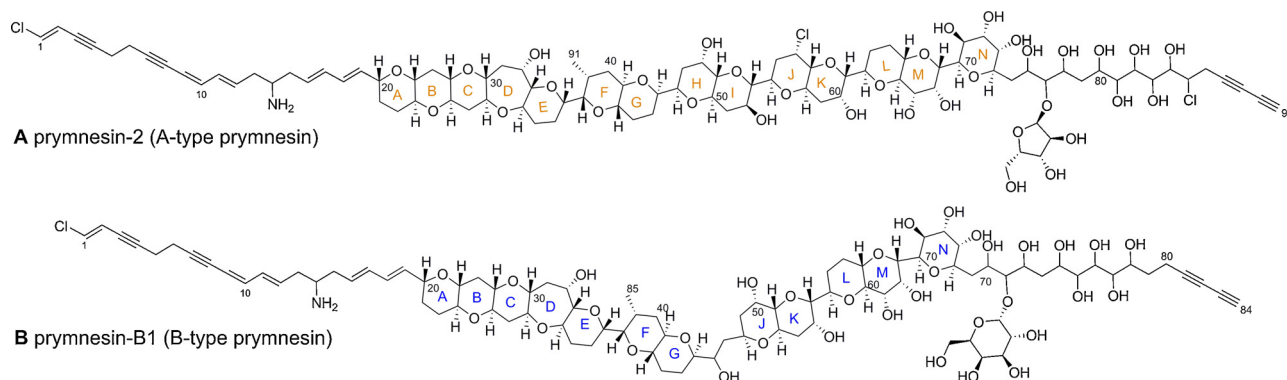
Fig. 1. The structures of A- and B-type prymnesins. (A) Structure of an A-type prymnesin, here prymnesin-2, note ring H and I, these have been replaced in the B-type by a single carbon-carbon bond; (B) Structure of a B-type prymnesin, here prymnesin-B1, notice the lack of ring-system H, I.

(Rasmussen et al., 2016b). The backbone structure of the C-type prymnesins has not been elucidated, whereas the backbone for both A- and B-type prymnesins is known (Fig. 1) (Igarashi et al., 1996, 1999; Rasmussen et al., 2016b). Variances within each type of prymnesin are found in degree of chlorination (one to four) and saturation (one or two double bonds more than the prymnesins structurally elucidated so far) and number of sugar moieties attached (zero to two pentose and/or hexose conjugates). Since chlorine is an A + 2 element, the isotopic pattern helped to determine the degree of chlorination of the individual molecular features. Attached sugar moieties were determined by consecutive in-source fragmentation down to the backbone structure in the HRMS-scan (see Fig. S2). Using this approach it is only possible to distinguish between pentose and hexose conjugates, but it is not possible to determine the exact nature of the attached sugars (e.g. ribofuranose, galactofuranose). This would require a purification of the compounds followed by hydrolysis and identification of the sugar moieties by e.g. gas chromatography coupled to mass spectrometry or nuclear magnetic resonance spectroscopic confirmation. Of the 26 screened strains of *P. parvum* 9 produced the A-type prymnesins, 6 the B-type, and 11 produced the C-type under the chosen cultivation conditions (see Table S2). None of the tested strains produced more than one type of prymnesin, however all strains were found to produce prymnesins.

Within the three types of prymnesins different sub-backbones could be classified varying in the degree of chlorination, degree of saturation and incorporated oxygen. Compared to the previous publication (Rasmussen et al., 2016b), the sub-backbones of A-type prymnesins doubled from two to four. Furthermore, two new B-type backbones and four new C-type sub-backbones could be tentatively identified based on HRMS-data increasing the total number to three (B-type) and nine (C-type) backbones. Together with the glycosylation patterns, a total of 51 different molecular features were identified (9 A-type, 12 B-type and 30 C-type prymnesins, see Table S3 and S4), which is three times more than the 16 molecular features described in Rasmussen et al. (2016b). The chemical diversity of prymnesins seems to be even significantly larger since each molecular feature was observed at least twice in the vast majority of samples. For example, in case of the strain K-0081, a B-type prymnesin producer, the molecular feature of the B-type backbone with one incorporated chlorine, one pentose and one hexose-unit was detected at 5.6, 5.8 (minor peaks) and 5.9 min (major peak). Differences in the retention time might be caused by different stereo-chemistries or by different sugar moieties of the same type (hexose or pentose) attached at different oxygenated positions of the core carbon chain or other structural isomers. Within the C-type prymnesins the largest diversity was observed, including some molecular features that could not be explained. Supplementary Figs. S3–S5 provide an overview of the molecular features used in this study to illustrate the complexity and diversity of each strain investigated.

3.2. Geographical distribution of P. parvum strains producing A-, B- and C-type prymnesins

The isolation site for each of the 26 strains included in the present study is illustrated on a world map and color-coded based on the type of prymnesin produced (Fig. 2). Strains of *P. parvum* producing either A-, B- or C-type of prymnesins showed a complex distribution pattern independent of the biogeography. In some areas, e.g. the European part of the Atlantic Ocean, strains representing all three types of prymnesins co-exist.

3.3. Phylogenetic inference

The internal transcribed spacer regions (ITS-1 and ITS-2) of the nuclear ribosomal cistron are known for their high sequence variability, why they are regularly used as markers for phylogenetic analyses of closely related taxa (i.e. species, populations). Here analyses of 26

strains of *P. parvum* with a wide geographical distribution used ITS-1–5.8S rDNA–ITS-2 sequences to reveal the relationship among these strains. The tree topology from Bayesian inference is illustrated as Fig. 3. Three main clades (color-coded) were recovered with either high (1.0 and 99%), moderate (0.77 and 87%) or low (0.53 and 56%) statistical support from Bayesian posterior probabilities and maximum likelihood bootstrap values, respectively. The *P. parvum* strains did not cluster according to a biogeographical distribution pattern. If this had been the case strains established from the same geographical area would have been expected to represent the same population (i.e. identical or similar ITS sequences). Similarly, strains originating from samples collected from different geographical areas would have been expected to be distantly related due to different ITS sequences. Surprisingly the strains of *P. parvum* clustered according to their type of prymnesins indicating that gene flow does not occur between clades even when co-existing (e.g. strains ARC83, ARC85 and ARC140 all from Elizabeth City, North Carolina, USA) and that an independent genetic structure apparently supports the production of different types of prymnesins. Furthermore, the phylogenetic inference indicates that strains of *P. parvum* producing A-type prymnesins (9 strains examined with a global distribution) and strains producing B-type prymnesins (6 strains examined mainly from northern Europe) form a sister group relationship and that both of these groups form a sister group to strains producing the C-type prymnesins (11 strains examined with a global distribution).

3.4. Sequence divergence

The three groups separated by type of prymnesin had very different within mean group distances calculated using MEGA version 7 (Kumar et al., 2016) and based on ITS-1–5.8SrDNA–ITS-2 (696 base pairs): A-type prymnesins: 0.1%; B-type prymnesins: 0% and C-type prymnesins: 1.7%. The larger genetic distance between strains with C-type prymnesins is also illustrated by the longer branch lengths compared to *P. parvum* strains characterized by possessing A- and B-type prymnesins (Fig. 3).

4. Discussion

4.1. Prymnesin production among P. parvum strains

In the present study 26 strains of *P. parvum* were screened for the production of prymnesins and all produced one type of prymnesin. Three different prymnesin types labelled A-, B- and C-type prymnesins could be distinguished, but all the individual strains only produced one type of prymnesins. Thus, the presented results with a larger data set reinforced the recent findings made by Rasmussen et al. (2016b). The A-type prymnesins were only observed in one strain at that time, suggesting that the strains producing A-type prymnesins might be rare or harder to isolate for culturing (Rasmussen et al., 2016b). This could not be confirmed in the present study. Out of the 26 *P. parvum* strains investigated, 9 strains produced A-type prymnesins, 6 produced B-type prymnesins, and 11 produced C-type prymnesins, indicating that all types of prymnesins are common and widely distributed.

The A-, B- and C-type prymnesins differ in the length of the carbon backbone of the compound. The existence of backbones having different sizes is not common among phycotoxins (Andersen et al., 2016). Among phycotoxins, the size of a backbone is usually fixed, whereas changes may occur to a number of sidechains or functional groups (like found in saxitoxins, karlotoxins, azaspiracids (Rasmussen et al., 2016a; Twiner et al., 2008; Van Wagoner et al., 2010; Place et al., 2012; Cusick and Sayler, 2013)). Apart from the prymnesins, only brevetoxins (type A and B) and gymnocins (type A and B) have this feature. These toxins are produced by the red-tide dinoflagellates *Karenia brevis* and *K. mikimotoi* (Rasmussen et al., 2016a).

Several analogs have been found within the different prymnesin
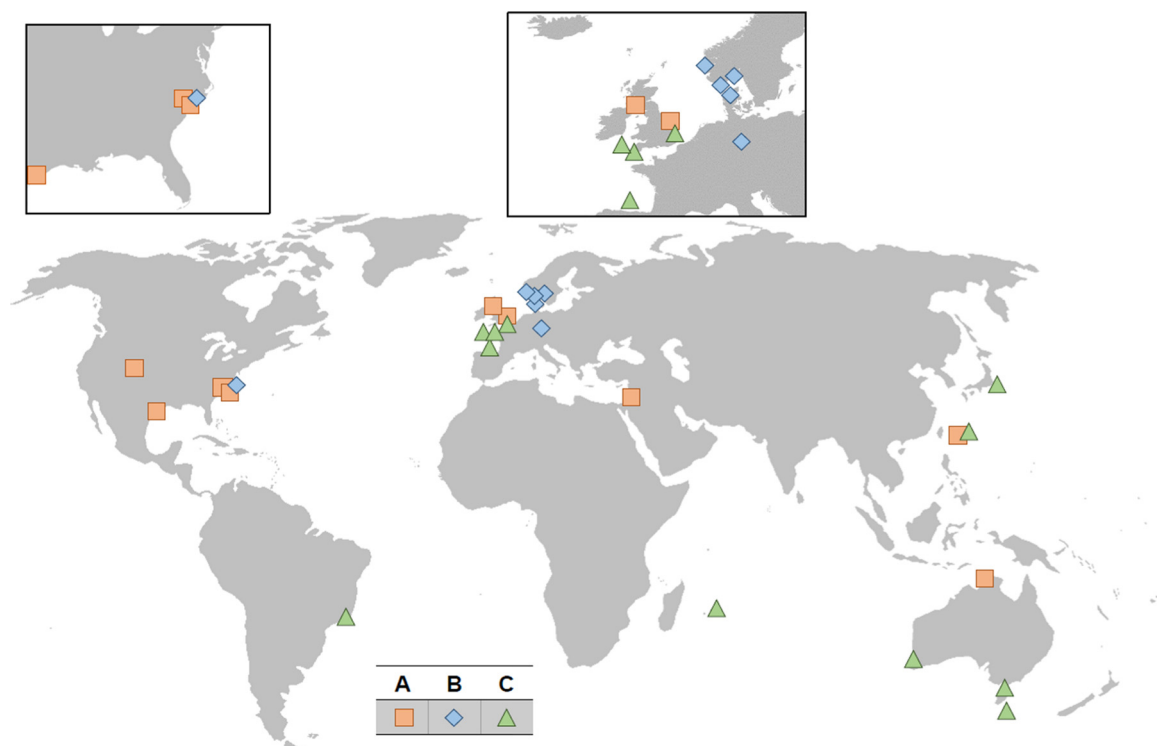
Fig. 2. Geographical distribution of *Prymnesium parvum* producing A-, B-, and C-type prymnesins investigated in this study according to the isolation side. Orange squares denote A-type, blue diamonds B-type, green triangles C-type prymnesins producers. (For interpretation of the references to colour in this figure legend, the reader is referred to the web version of this article).
(Map modified after: world map: E Pluribus Anthony, version of June 19th 2006, https://commons.wikimedia.org/wiki/File:BlankMap-World-noborders.png (accessed June 14th 2018), Europe map: Roke ~ commonswiki, version of May 2nd 2007, https://commons.wikimedia.org/wiki/File:BlankMap-Europe-v3.png (accessed June 14th 2018), and US map: Lokal_Profil, version of June 27th 2007, https://commons.wikimedia.org/wiki/File:Blank_US_Map,_Mainland_with_no_States.svg (accessed June 14th 2018)).
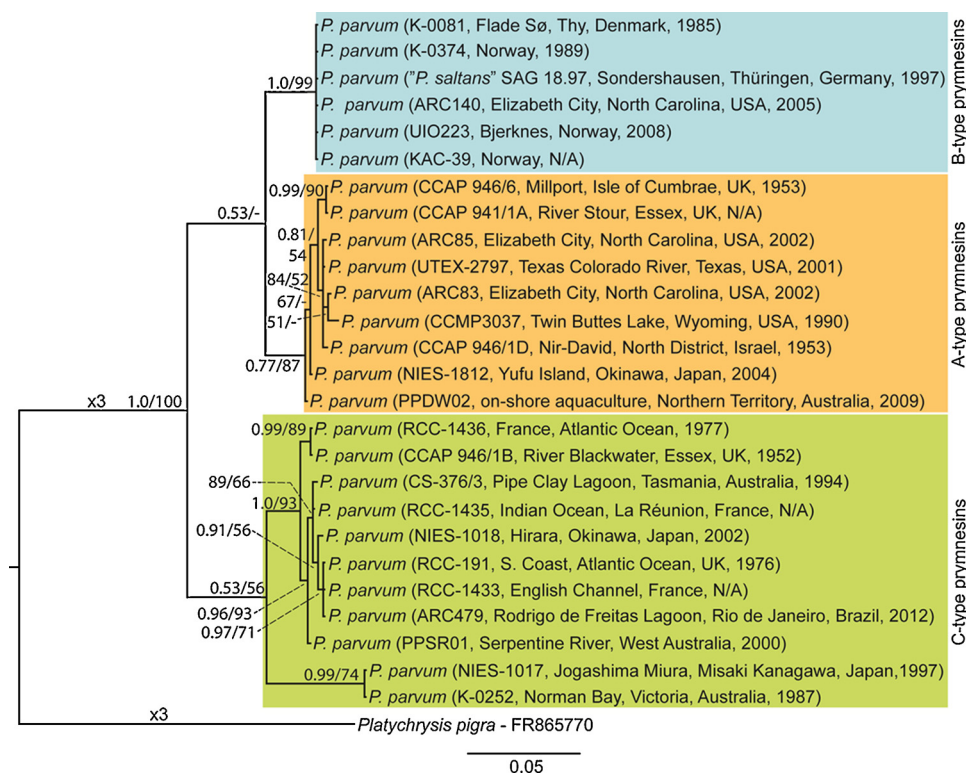
Fig. 3. Phylogeny of 26 widely distributed strains of *Prymnesium parvum* inferred from Bayesian analysis. Analysis was based on 696 base pairs (including introduced gaps) of internal transcribed spacers (ITS-1 and ITS-2) and the 5.8S rDNA gene. *Platychrysis pigra* was used as outgroup. Numbers at internal nodes are posterior probabilities (≥ 0.5) from Bayesian analysis followed by bootstrap values (≥ 50%) from maximum likelihood with 1 000 replications. Strain numbers and geographical origin are provided for all sequences. Branch lengths are proportional to the number of character changes.

types in *P. parvum*, (Rasmussen et al. (2016b) and the present study) varying in chlorination (one to four), degree of saturation and number of sugar moieties attached (zero to two pentose and/or hexose units). Hems et al. (2018) reported two new B-type prymnesins, which were also found in the current study (PRM-B (2 Cl) and PRM-B (2 Cl) + hexose). It is seen critical that they named these two compounds prymnesin-B6 and -B7 because exact naming of natural products should only be provided if a full structural elucidation, including at least relatively stereochemical assessment, is in place. To facilitate discussions in the present manuscript systematic names are proposed which are based on mass spectrometric characterization. Furthermore, Hems et al. (2018) reported a new type of prymnesins (D-type) containing 85 carbon atoms in the aglycone backbone part of the compounds. Based on the previously proposed classification on the number of carbon atoms in the backbone (Rasmussen et al. 2016) these do not represent an entirely new type, but are instead only previously not reported variations of B-type prymnesins.

To what extent the composition of the analogs, produced by a given strain, is fixed or can be affected by cultivation conditions is presently unknown. It should be also noted here that all strains were cultivated only under one growth condition and that samples were harvested in the late exponential growth phase. Therefore, it might be possible that some analogs only produced under specific conditions or in a specific growth phase were overlooked.

Studies on variability of toxin production in the dinoflagellates *Alexandrium* spp. and *K. veneficum* indicate that the suite of toxin analogs produced is strain specific and not affected by environmental factors. The total amount of toxins and composition of analogs produced can however be affected by environmental factors such as salinity, growth phase, media compositions (Place et al., 2012; Lim and Ogata, 2005; Otero et al., 2010; Medhioub et al., 2011; Suikkanen et al., 2013) and changes in CO_2 levels (Fu et al., 2010). Furthermore, abiotic factors such as the presence of grazer or their cues might affect toxin production, as shown for e.g. cyanobacteria (Jang et al., 2003), diatoms (Harðardóttir et al., 2015) and dinoflagellates (Selander et al., 2014).

4.2. A biogeographical pattern does not exist with regard to the different types of prymnesins

The biogeographical distribution of the analyzed strains showed limited clustering of prymnesin types, with A-type producing strains being most frequent in North America, but also present in the rest of the world, and B-type producing strains being dominant in Scandinavian waters, but also present in North America. The C-type prymnesins were present in the northern and southern hemisphere, but were not detected in North America. As more strains are analyzed these tendencies may be subject to change. The results presented here are thus well in line with the observation made by Rasmussen et al. (2016b).

Distinct differences in biogeography among toxic microalgae and their toxins have been observed in some cases previously. It has been shown for instance in the case of *K. veneficum* that frequently blooms on the east coast of the US (Lin et al., 2018). In the Chesapeake Bay, karlotoxin-1 is the predominant toxin type, while outside the Bay, along the Atlantic coast of US, Australia, and China karlotoxin-2 is the predominant toxin type (Place et al., 2012; Bachvaroff et al., 2009; Dai et al., 2014; Adolf et al., 2015). Biogeographical differences have also been detected in *Alexandrium ostenfeldii*. In this dinoflagellate species strains from low salinity (Baltic sea) waters produce paralytic shellfish toxins only, while strains from oceanic waters (Mediterranean Sea, Northern Atlantic coast of Canada and US) produce spirolides only. Strains from areas with intermediate salinity (Danish Straits) produce both types of toxins (Suikkanen et al., 2013). No such tendencies were observed for *P. parvum*, where both A- and B-type prymnesin producing strains have been observed in inland lakes and both A- and B-type prymnesin producing strains have been isolated from the same location (Elizabeth City, NC, USA).

4.3. The production of A-, B- and C-type prymnesins is related to phylogeny of P. parvum

In previous publications two and three major clades within *P. parvum* were identified based on ITS-sequences (Larsen and Medlin, 1997; Lutz-Carrillo et al., 2010, respectively). This observation was supported by the present phylogenetic analyses, which revealed three major clades. Interestingly, the clades matched the distribution of prymnesin types and no evident biogeographic clustering was observed. Such link between chemotype and phylotype has never been reported before for a HAB-forming alga. The statistical support for the branching pattern of clades varied though from high support (strains with B-type prymnesins) to moderate support for strains with A-type prymnesins and rather low support for strains with C-type prymnesins. The support for the branching pattern of prymnesins was only weakly supported. Yet, if this branching pattern matches the true evolution of prymnesins, then the C-type might represent the ancestral state from which both A- and B-type prymnesin producing strains evolved. This may reflect an evolutionary selection pressure towards producing increasingly more toxic compounds as prymnesin-2 (an A-type prymnesin) is even more toxic than prymnesin-B1 (a B-type prymnesin (Rasmussen et al., 2016b)) in a rainbow trout gill cell assay. Additional genetic markers (e.g. microsatellites) should be established to better understand, which the earliest branching prymnesin type is.

The question then arises, what drives increased levels of toxicity? One obvious answer could be competition for resources (increased fitness due to effects of allelopathy) between populations occurring in the same geographical area. The much larger sequence divergence within C-type prymnesin producing strains (1.7%) compared to strains with A-type (0.1%) or B-type (0%) may reflect their ancestral status (i.e. longer evolutionary history). Alternatively, the earliest diverging strains NIES-1017 and K-0252 may represent a subtype of the C-type prymnesins and thus explaining the large within group divergence when including all strains. Further analyses of the chemical structure of C-type prymnesins will have to reveal if a subdivision within this group can be justified.

4.4. Biosynthesis of prymnesins in the context of evolution

For two decades only prymnesin-1 and prymnesin-2 were known from *P. parvum* (Igarashi et al., 1996, 1999). Therefore, it is striking that the chemical diversity of prymnesins is as high as demonstrated here. Especially, since the reported detection of 51 different prymnesins defined by their molecular formulas (9 A-type, 12 B-type, and 30 C-type prymnesins, Tables S3 and S4) does not even include structural isomers. Such a high chemical diversity, and the fact that all 26 investigated strains produce prymnesins, strongly indicates that a flexible capability of being able to produce, and even evolve these allelochemicals (phycotoxins) into more toxic variants, likely provide *P. parvum* with a competitive advantage over other microalgal species and other marine organisms in natural environments.

Prymnesins are classified as supersized ladder-like polyethers, in which the core part of the molecule resembles the structures of other algal ladder-frame polyether toxins such as ciguatoxins, brevetoxins and gymnocins, known from *Gambierdiscus polysiensis*, *K. brevis* and *K. mikimotoi*, respectively (Rasmussen et al., 2016a). It is commonly accepted that the core part of these compounds are derived from long and highly reduced polyketide chains containing numerous double bond (derived from ketoreductase and dehydratase activities) (Van Wagoner et al., 2014). Subsequent polyepoxidation and polyether formation (catalyzed by epoxide hydrolases) creates the core structures of e.g. prymnesins that are then further modified by tailoring enzymes (halogenation, glycosylation) to increase the chemodiversity. Currently, not much is known about the underlying mechanisms for polyketide biosynthesis in the haptophyte *P. parvum*. Experiments with physiological shock treatments of *P. parvum* have demonstrated that increased toxicity could be related to higher copy numbers of selected

uncharacterized polyketide synthase (PKS) genes suggesting a connection between toxicity and the PKS biosynthetic pathway (Freitag et al., 2011). On the other hand, recent studies have demonstrated that unique modular type I PKSs are indeed involved in the biosynthesis of polyethers in dinoflagellates such as *K. brevis* (Monroe et al., 2010), *K. mikimotoi* (Kimura et al., 2015) and species in the genus *Gambierdiscus* (Kohli et al., 2015, 2017). In line with these findings, and the partly structural similarities between brevetoxins, gymnocins and prymnesins, it is speculated that evolution of similar type of genes encoding modular type I PKSs in *P. parvum* have evolved by gene duplications. In this way an original C-type prymnesin, having an 83 carbon long polyketide backbone, might have evolved into the longer B-type (85 carbon atoms), by addition of just one extra acetate extender unit (e.g. incorporated driven by decarboxylation of malonyl-coenzyme A) to the initial growing polyketide chain. Similarly, A-type prymnesins (91 carbon atoms) could be derived from further gene duplications, leading to addition of four acetate extender units to the original C-type prymnesins. This hypothesis is neither supported or can be rejected by the phylogenetic inferences conducted here as the branching pattern of the prymnesin type lineages could not be determined with confidence (Fig. 3). Hence, it could be that strains producing the C-type prymnesins represent the ancestral type of *P. parvum*. The fact that 30 variants (9 sub-backbones) of C-type prymnesins were detected and only 12 (4 sub-backbones) and 9 variants (3 sub-backbones) of the B- and A-type prymnesins, respectively, could also indicate that minor structural changes (e.g. in chlorination, reduction, oxidation and glycosylation patterns) have had longer time to evolve, explaining the larger intratype chemodiversity seen for the C-type prymnesins.

4.5. Is it valid to split P. parvum into at least three species using chemotaxonomy and ITS-type classification?

Traditionally identification of species of *Prymnesium* is based on fine structural differences of both the proximal and distal sides of organic, oval scales arranged in layers around the cell body (Moestrup and Larsen, 1992). This has resulted in the description of 24 species of *Prymnesium* (Guiry and Guiry, 2018). Using internal transcribed spacers and the 5.8S rDNA gene, the sequence divergence between all pairwise comparisons of prymnesin types ranged from 3.2 to 4.3% (A- and B-type B: 3.2%; A- and C-type: 3.6%; B- and C-type: 4.3%). Thus, the presented findings challenge the morphological species concept by revealing not only a consistent genotypic (different DNA sequences), but also a phenotypic (prymnesin type) difference between strains. Using chemotaxonomy and ITS-type classification arguments favor the splitting of *P. parvum* into two additional species. To formally erect new species of *Prymnesium* is however not possible before additional sequencing data and careful studies of body scales have been conducted for all strains. Further studies should include both small subunit (SSU) and large subunit (LSU) rDNA sequences for which only two SSU and six partial LSU rDNA sequences are currently available.

A recent study of 99 strains of the haptophyte *Emiliania huxleyi* using a multigene approach combining nuclear, chloroplast and mitochondrial gene sequences also revealed the likely existence of cryptic species within *Emiliania*, which otherwise is a morphologically well-defined species (Bendif et al., 2014). Similarly, the combined use of rDNA LSU and ITS as genetic markers, were demonstrated to divide strains of *K. mikimotoi* from different geographical regions into distinct sub-groups (Al-Kandari et al., 2011), however a correlation to chemotypes was not included. Recent studies of the *Alexandrium tamarense* complex and the green alga *Micromonas pusilla* also showed that morphology did not completely match genetic divergence and thus resulted in a revision of the genera and erection of new species (John et al., 2014; Simon et al., 2017). Hence, at least five studies (including this one) based on high numbers of strains have shown a genetic diversity previously masked by morphology. Future studies will have to verify the presence of additional cryptic species of small-sized protists.

4.6. Future identification of bloom forming Prymnesium

Based on the presented findings the use of morphological characters to identify the apparently cryptic *P. parvum* is problematic. Correct identification has become of paramount importance since prymnesins differ in toxicity (e.g. prymnesin-2 (A-type) is six times more toxic than prymnesin-B1 (B-type) in a rainbow trout gill cell assay; (Rasmussen et al., 2016b)) and blooms may therefore have a very different impact on the environment. In the future, prymnesins might be used as chemotaxonomic markers. With the data presented here, identification of prymnesin types can be achieved either by conducting a chemical analysis using LC-DAD-HRMS or by determining the ITS sequence due to the evidence of clade specific compound production. Even fast enumeration of cell abundance in bloom forming populations comprising different prymnesin types is possible following the design of specific primers and hydrolysis probes for use in real-time qPCR assays (Eckford-Soper and Daugbjerg, 2015). Altogether, this study demonstrates a clear link between genotyping and chemotyping in microalgae that are in practice impossible to differentiate based on morphological taxonomy. The presented findings could potentially set the scene for a paradigm shift towards a more polyphasic taxonomic approach for identification of important toxic microalgae, similar to what has been implemented for other eukaryotic organisms such as filamentous fungi (Frisvad and Samson, 2004).

Conflict of interest

The authors declare no conflict of interest.

Author contributions

S.B.B., D.K.S., E.P., P.J.H., T.O.L. and E.V. conceived and designed the screening experiments. S.B.B. cultivated the algae, whereas D.K.S. was primarily responsible for the chemical analysis. N.D. conceived, designed and performed the PCR-analysis. C.A-d-S. cultivated and provided the Brazilian strain. P.J.H., T.O.L. and E.V. supervised the experimental work. S.B.B., D.K.S., N.D., P.J.H., T.O.L. and E.V. wrote and all authors amended and corrected the paper.

Acknowledgements

Appendix A. Supplementary data

Supplementary material related to this article can be found, in the online version, at doi:https://doi.org/10.1016/j.hal.2018.11.010.

References

Adolf, J.E., Bachvaroff, T.R., Deeds, J.R., Place, A.R., 2015. Ichthyotoxic *Karlodinium veneficum* (Ballantine) J Larsen in the Upper Swan River estuary (Western Australia):

ecological conditions leading to a fish kill. Harmful Algae 48, 83–93.

Al-Kandari, M.A., Highfield, A.C., Hall, M.J., Hayes, P., Schroeder, D.C., 2011. Molecular tools separate harmful algal bloom species, *Karenia mikimotoi*, from different geographical regions into distinct sub-groups. Harmful Algae 10, 636–643.

Alves-De-Souza, C., Benevides, T.S., Santos, J.B.O., von Dassow, P., Guillou, L., Menezes, M., 2017. Does environmental heterogeneity explain temporal β diversity of small eukaryotic phytoplankton? Example from a tropical eutrophic coastal lagoon. J. Plankton Res. 39, 698–714.

Andersen, A.J.C., Hansen, P.J., Jørgensen, K., Nielsen, K.F., 2016. Dynamic Cluster Analysis: an unbiased method for identifying A + 2 element containing compounds in liquid chromatographic high-resolution time-of-flight mass spectrometric data. Anal. Chem. 88, 12461–12469.

Anderson, D.M., Hoagland, P., Kaoru, Y., White, A.W., 2000. Estimated annual economic impacts from harmful algal blooms (HABs) in the United States. Technical Report WHOI-2000-11. . (Last Accessed 5th August 2018). http://www.whoi.edu/cms/files/Economics_report_18564_23050.pdf.

Bachvaroff, T.R., Adolf, J.E., Place, A.R., 2009. Strain variation in *Karlodinium veneficum* (Dinophyceae): toxin profiles, pigments, and growth characteristics. J. Phycol. 45, 137–153.

Bendif, E.M., Probert, I., Carmichael, M., Romac, S., Hagino, K., de Vargas, C., 2014. Genetic delineation between and within the widespread coccolithophore morphospecies *Emiliania huxleyi* and *Gephyrocapsa oceanica* (Haptophyta). J. Phycol. 50, 140–148.

Berge, T., Poulsen, L.K., Moldrup, M., Daugbjerg, N., Hansen, P.J., 2012. Marine microalgae attack and feed on metazoans. ISME J. 6, 1926–1936.

Cusick, K.D., Sayler, G.S., 2013. An overview on the marine neurotoxin, saxitoxin: genetics, molecular targets, methods of detection and ecological functions. Mar. Drugs 11, 991–1018.

Dai, X., Lu, D., Guan, W., Wang, H., He, P., Xia, P., Yang, H., 2014. Newly recorded *Karlodinium veneficum* dinoflagellate blooms in stratified water of the East China Sea. Deep Sea Res. Part II: Top Stud. Oceanogr. 101, 237–243.

Darriba, D., Taboada, G.L., Doallo, R., Posada, D., 2012. jModelTest2: more models, new heuristics and parallel computing. Nat. Methods 9, 772.

Eckford-Soper, L.K., Daugbjerg, N., 2015. Development of a multiplex real-time qPCR assay for simultaneous enumeration of up to four marine toxic bloom-forming microalgal species. Harmful Algae 48, 37–43.

Edvardsen, B., Paasche, E., 1998. Bloom dynamics and physiology of *Prymnesium* and *Chrysochromulina*. In: Anderson, D.M., Cembella, A.D., Hallegraeff, G.M. (Eds.), Physiological Ecology of Harmful Algal Blooms. Springer-Verlag, Berlin pp 193–208.

Freitag, M., Beszteri, S., Vogel, H., John, U., 2011. Effects of physiological shock treatments on toxicity and polyketide synthase gene expression in *Prymnesium parvum* (Prymnesiophyceae). Eur. J. Phycol. 46, 193–201.

Frisvad, J.C., Samson, R.A., 2004. Polyphasic taxonomy of *Penicillium* subgenus *Penicillium* - a guide to identification of food and air-borne terverticillate Penicillia and their mycotoxins. Stud. Mycol. 49, 1–173.

Fu, F.X., Place, A.R., Garcia, N.S., Hutchins, D.A., 2010. CO_2 and phosphate availability control the toxicity of the harmful bloom dinoflagellate *Karlodinium veneficum*. Aquat. Microb. Ecol. 59, 55–65.

Guillard, R.R.L., 1975. Culture of Phytoplankton for Feeding marine Invertebrates. In: Smith, W.L., Chanley, M.H. (Eds.), Culture of Marine Invertebrate Animals. Springer, Boston pp 29–60.

Guindon, S., Dufayard, J.-F., Lefort, V., Anisimova, M., Hordijk, W., Gascuel, O., 2010. New algorithms and methods to estimate maximum-likelihood phylogenies: assessing the performance of PhyML 3.0. Syst. Biol. 59, 307–321.

Guiry, M.D., Guiry, G.M., 2018. AlgaeBase. World-wide electron publication. National University of Ireland, Galway . (Last Accessed on 5th August 2018). http://www.algaebase.org/search/genus/detail/?genus_id=B610b4c83475e18e5.

Harðardóttir, S., Pančić, M., Tammilehto, A., Krock, B., Møller, E.F., Nielsen, T.G., Lundholm, N., 2015. Dangerous relations in the arctic marine food web: Interactions between toxin producing *Pseudo-nitzschia* diatoms and *Calanus* copepodites. Mar. Drugs 13, 3809–3835.

Hems, E.S., Wagstaff, B.A., Saalbach, G., Field, R.A., 2018. CuAAC click chemistry for enhanced detection of novel alkyne-based natural product toxins. Chem. Commun. 54, 12234.

Ianora, A., Bentley, M.G., Caldwell, G.S., Casotti, R., Cembella, A.D., Engström-Öst, J., Halsband, C., Sonnenschein, E., Legrand, C., Llewellyn, C.A., Paldavičiene, A., Pilkaityte, R., Pohnert, G., Razinkovas, A., Romano, G., Tillmann, U., Vaiciute, D., 2011. The relevance of marine chemical ecology to plankton and ecosystem function: an emerging field. Mar. Drugs 9, 1625–1648.

Igarashi, T., Satake, M., Yasumoto, T., 1996. Prymnesin-2: a potent ichthyotoxic and hemolytic glycoside isolated from the red tide alga Prymnesium parvum. J. Am. Chem. Soc. 118, 479–480.

Igarashi, T., Satake, M., Yasumoto, T., 1999. Structures and partial stereochemical assignments for prymnesin-1 and prymnesin-2: potent hemolytic and ichthyotoxic glycosides isolated from the red tide alga *Prymnesium parvum*. J. Am. Chem. Soc. 121, 8499–8511.

Jang, M.-H., Ha, K., Joo, G.-J., Takamura, N., 2003. Toxin production of cyanobacteria is increased by exposure to zooplankton. Freshwater Biol. 48, 1540–1550.

John, U., Litaker, R.W., Montresor, M., Murray, S., Brosnahan, M.L., Anderson, D.M., 2014. Formal revision of the *Alexandrium tamarense* species complex (Dinophyceae) taxonomy: the introduction of five species with emphasis on molecular-based (rDNA) classification. Protist 165, 779–804.

Jonsson, P.R., Pavia, H., Toth, G., 2009. Formation of harmful algal blooms cannot be explained by allelopathic interactions. Proc. Natl. Acad. Sci. U. S. A 106, 11177–11182.

Kaartvedt, S., Johnsen, T.M., Aksnes, D.L., Lie, U., Svendsen, H., 1991. Occurrence of the toxic phytoflagellate *Prymnesium parvum* and associated fish mortality in a Norwegian fjord. Can. J. Fish Aquat. Sci. 48, 2316–2323.

Kimura, K., Okuda, O., Nakayama, K., Shikata, T., Takahashi, F., Yamaguchi, H.,

Skamoto, S., Yamaguchi, M., Tomaru, Y., 2015. RNA sequencing revealed numerous polyketide synthase genes in the harmful dinoflagellate *Karenia mikimotoi*. PLoS One 10, e0142731.

Kohli, G.S., John, U., Figueroa, R.I., Rhodes, L.L., Harwood, D.T., Groth, M., Bolch, C.J.S., Murray, S.A., 2015. Polyketide synthesis genes associated with toxin production in two species of *Gambierdiscus* (Dinophyceae). BMC Genomics 16, 410.

Kohli, G.S., Campbell, K., John, U., Smith, K.F., Fraga, S., Rhodes, L.L., Murray, S.M., 2017. Role of modular polyketide synthases in the production of polyether ladder compounds in ciguatoxin-producing *Gambierdiscus polynesiensis* and *G. excentricus* (Dinophyceae). J. Eukaryot. Microbiol. 64, 691–706.

Kumar, S., Stecher, G., Tamura, K., 2016. MEGA7: Molecular Evolutionary Genetics Analysis version 7.0 for bigger datasets. Mol. Biol. Evol. 33, 1870–1874.

Larsen, A., Medlin, L.K., 1997. Inter- and intraspecific genetic variation in twelve *Prymnesium* (Haptophyceae) clones. J. Phycol. 33, 1007–1015.

Lim, P.T., Ogata, T., 2005. Salinity effect on growth and toxin production of four tropical *Alexandrium species* (Dinophyceae). Toxicon 45, 699–710.

Lin, C.H., Lyubchich, V., Glibert, P.M., 2018. Time series models of decadal trends in the harmful algal species *Karlodinium veneficum* in Chesapeake Bay. Harmful Algae 73, 110–118.

Lutz-Carrillo, D.J., Southard, G.M., Fries, L.T., 2010. Global genetic relationships among isolates of golden alga (*Prymnesium parvum*). J. Am. Water Resour. Assoc. 46, 24–32.

Medhioub, W., Sechet, V., Truquet, P., Bardouil, M., Amzil, Z., Lassus, P., Soudant, P., 2011. *Alexandrium ostenfeldii* growth and spirolide production in batch culture and photobioreactor. Harmful Algae 10, 794–803.

Moestrup, Ø., Larsen, J., 1992. Potentially toxic phytoplankton 1. Haptophyceae (Prymnesiophyceae) ICES Identification Leaflets for Plankton Leaflet No. 179. . (Last Accessed on 5th August 2018). http://www.ices.dk/sites/pub/Publication%20Reports/Plankton%20leaflets/SHEET179.PDF.

Monroe, E.A., Johnson, J.G., Wang, Z., Pierce, R.K., Van Dolah, F.M., 2010. Characterization and expression of nuclear-encoded polyketide synthases in the brevetoxin-producing dinoflagellate *Karenia brevis*. J. Phycol. 46, 541–552.

Otero, P.A.Z., Alfonso, A., Vieytes, M.R., Cabado, A.G., Vieites, J.M., Botana, L.M., 2010. Effects of environmental regimens on the toxin profile of *Alexandrium ostenfeldii*. Environ. Toxicol. Chem. 29, 301–310.

Peng, J., Place, A.R., Yoshida, W., Anklin, C., Hamann, M.T., 2010. Structure and absolute configuration of karlotoxin-2, an ichthyotoxin from the marine dinoflagellate *Karlodinium veneficum*. J. Am. Chem. Soc. 132, 3277–3279.

Place, A.R., Bowers, H.A., Bachvaroff, T.R., Adolf, J.E., Deeds, J.R., Sheng, J., 2012. *Karlodinium veneficum* – the little dinoflagellate with a big bite. Harmful Algae 14, 179–195.

Rasmussen, S.A., Andersen, A.J.C., Andersen, N.G., Nielsen, K.F., Hansen, P.J., Larsen, T.O., 2016a. Chemical diversity, origin, and analysis of phycotoxins. J. Nat. Prod. 79, 662–673.

Rasmussen, S.A., Meier, S., Andersen, N.G., Blossom, H.E., Duus, J.Ø., Nielsen, K.F., Hansen, P.J., Larsen, T.O., 2016b. Chemodiversity of ladder-frame prymnesin polyethers in *Prymnesium parvum*. J. Nat. Prod. 79, 2250–2256.

Rasmussen, S.A., Binzer, S.B., Hoeck, C., Meier, S., de Medeiros, L.S., Andersen, N.G., Place, A., Nielsen, K.F., Hansen, P.J., Larsen, T.O., 2017. Karmitoxin: an amine-containing polyhydroxy-polyene toxin from the marine dinoflagellate *Karlodinium armiger*. J. Nat. Prod. 80, 1287–1293.

Ronquist, F., Huelsenbeck, J.P., 2003. MrBayes 3: Bayesian phylogenetic inference under mixed models. Bioinformatics 19, 1572–1574.

Sanseverino, I., Conduto, D., Pozzoli, L., Dobricic, S., Lettieri, T., 2016. Algal bloom and its economic impact. JRC Technical Reports EUR 27905 EN. https://doi.org/10.2788/660478.

Selander, E., Kubanek, J., Hamberg, M., Andersson, M.X., Cervin, G., Pavia, H., 2014. Predator lipids induce paralytic shellfish toxins in bloom-forming algae. Proc. Natl. Acad. Sci. U. S. A. 112, 6395–6400.

Simon, N., Foulon, E., Grulois, D., Six, C., Desdevises, Y., Latimier, M., Le Gal, F., Tragin, M., Houdan, A., Derelle, E., Jouenne, F., Marie, D., Le Panse, S., Vaulot, D., Marin, B., 2017. Revision of the genus *Micromonas* Manton et Parke (Chlorophyta, Mamiellophyceae), of the type species *M. pusilla* (Butcher) Manton & Parke and of the species *M. commoda* van Baren, Bachy and Worden and description of two new species based on the genetic and phenotypic characterization of cultured isolates. Protist 168, 612–635.

Suikkanen, S., Kremp, A., Hautala, H., Krock, B., 2013. Paralytic shellfish toxins or spirolides? The role of environmental and genetic factors in toxin production of the *Alexandrium ostenfeldii* complex. Harmful Algae 26, 52–59.

Tillmann, U., 2003. Kill and eat your predator: a winning strategy of the planktonic flagellate *Prymnesium parvum*. Aquat. Microb. Ecol. 32, 73–84.

Twiner, M.J., Rehmann, N., Hess, P., Doucette, G.J., 2008. Azaspiracid shellfish poisoning: a review on the chemistry, ecology, and toxicology with an emphasis on human health impacts. Mar. Drugs 6, 39–72.

Van Wagoner, R.M., Deeds, J.R., Satake, M., Ribeiro, A.A., Place, A.R., Wright, J.L.C., 2008. Isolation and characterization of karlotoxin 1, a new amphipathic toxin from *Karlodinium veneficum*. Tetrahedron Lett. 49, 6457–6461.

Van Wagoner, R.M., Deeds, J.R., Tatters, A.O., Place, A.R., Tomas, C.R., Wright, J.L.C., 2010. Structure and relative potency of several karlotoxins from *Karlodinium veneficum*. J. Nat. Prod. 73, 1360–1365.

Van Wagoner, R.M., Satake, M., Wright, J.L.C., 2014. Polyketide biosynthesis in dinoflagellates: what makes it different? Nat. Prod. Rep. 31, 1101–1137.

Waterhouse, A.M., Procter, J.B., Martin, D.M.A., Clamp, M., Barton, G.J., 2009. Jalview version 2 – a multiple sequence alignment editor and analysis workbench. Bioinformatics 25, 1189–1191.

White, T.J., Bruns, T., Lee, S., Taylor, J., 1990. Amplification and direct sequencing of fungal ribosomal RNA genes for phylogenetics. In: Innis, M.A., Gelfand, D.H., Sninsky, J.J., White, T.J. (Eds.), PCR Protocols: A Guide to Methods and Applications. Academic Press Inc., New York pp 315–322.